



# Using polycyclic aromatic hydrocarbons for graphene growth on Cu(111) under ultra-high vacuum

Cite as: Appl. Phys. Lett. **121**, 191603 (2022); doi: [10.1063/5.0122914](https://doi.org/10.1063/5.0122914)

Submitted: 26 August 2022 · Accepted: 23 October 2022 ·

Published Online: 10 November 2022



View Online



Export Citation



CrossMark

Benedikt P. Klein,<sup>1,2</sup>  Matthew A. Stoodley,<sup>1,2</sup>  Matthew Edmondson,<sup>3</sup>  Luke A. Rochford,<sup>1</sup> Marc Walker,<sup>4</sup>  Lars Sattler,<sup>5</sup> Sebastian M. Weber,<sup>5</sup> Gerhard Hilt,<sup>5</sup>  Leon B. S. Williams,<sup>1,6,7</sup>  Tien-Lin Lee,<sup>1</sup> Alex Saywell,<sup>3</sup>  Reinhard J. Maurer,<sup>2,a)</sup>  and David A. Duncan<sup>1,a)</sup> 

## AFFILIATIONS

<sup>1</sup>Diamond Light Source, Harwell Science and Innovation Campus, Didcot OX11 0DE, United Kingdom

<sup>2</sup>Department of Chemistry, University of Warwick, Gibbet Hill Road, Coventry CV4 7AL, United Kingdom

<sup>3</sup>School of Physics and Astronomy, University of Nottingham, University Park, Nottingham NG7 2RD, United Kingdom

<sup>4</sup>Department of Physics, University of Warwick, Gibbet Hill Road, Coventry CV4 7AL, United Kingdom

<sup>5</sup>Institut für Chemie, Carl von Ossietzky Universität Oldenburg, Carl-von-Ossietzky-Straße 9-11, 26111 Oldenburg, Germany

<sup>6</sup>School of Chemistry, University of Glasgow, University Avenue, Glasgow G12 8QQ, United Kingdom

<sup>7</sup>School of Physics and Astronomy, University of Glasgow, University Avenue, Glasgow G12 8QQ, United Kingdom

<sup>a)</sup> Authors to whom correspondence should be addressed: [david.duncan@diamond.ac.uk](mailto:david.duncan@diamond.ac.uk) and [r.maurer@warwick.ac.uk](mailto:r.maurer@warwick.ac.uk)

## ABSTRACT

Ultra-high vacuum deposition of the polycyclic aromatic hydrocarbons azupyrene and pyrene onto a Cu(111) surface held at a temperature of 1000 K is herein shown to result in the formation of graphene. The presence of graphene was proven using scanning tunneling microscopy, x-ray photoelectron spectroscopy, angle-resolved photoemission spectroscopy, Raman spectroscopy, and low energy electron diffraction. The precursors, azupyrene and pyrene, are comparatively large aromatic molecules in contrast to more commonly employed precursors like methane or ethylene. While the formation of the hexagonal graphene lattice could naively be expected when pyrene is used as a precursor, the situation is more complex for azupyrene. In this case, the non-alternant topology of azupyrene with only 5- and 7-membered rings must be altered to form the observed hexagonal graphene lattice. Such a rearrangement, converting a non-alternant topology into an alternant one, is in line with previous reports describing similar topological alterations, including the isomerization of molecular azupyrene to pyrene. The thermal synthesis route to graphene, presented here, is achievable at comparatively low temperatures and under ultra-high vacuum conditions, which may enable further investigations of the growth process in a strictly controlled and clean environment that is not accessible with traditional precursors.

© 2022 Author(s). All article content, except where otherwise noted, is licensed under a Creative Commons Attribution (CC BY) license (<http://creativecommons.org/licenses/by/4.0/>). <https://doi.org/10.1063/5.0122914>

Industrial production of graphene worldwide is rising rapidly with currently ~10 000 tonnes produced annually.<sup>1</sup> However, the quality of mass-produced graphene is often comparatively low with small domain sizes and a high density of defects. The highest quality graphene films thus far achieved are grown via chemical vapor deposition (CVD) on metal substrates,<sup>2,3</sup> relying upon the catalytic activity of the substrate surface to crack C-H bonds in organic precursor molecules and to facilitate formation of a two-dimensional carbon film.

In this regard, copper as a substrate has been very popular.<sup>1,4</sup> It is a relatively cheap metal that can easily be made into a foil for roll-to-roll

processing and is, thus, one of the most common substrates for industrial scale CVD graphene growth.<sup>2</sup> However, standard methodologies of growing epitaxial graphene (e.g., CVD utilizing methane, ethane, or ethylene) require annealing temperatures<sup>5-7</sup> of the copper substrate close to its melting point (1358 K<sup>8</sup>). At such temperatures and under high vacuum pressures, copper itself has a notable vapor pressure<sup>5,9</sup> disrupting film growth.<sup>9</sup> To suppress this effect, it is necessary to use comparatively high pressures (~1 mbar)<sup>5,7</sup> during growth. Developing a method of producing high quality graphene at lower pressures and lower temperatures is, therefore, a worthwhile aim with significant potential for industrial applications.

Furthermore, despite the importance of studying graphene grown on copper, there are relatively few fundamental studies that have been performed on this system exploiting high precision surface science and nanotechnology techniques. While current methods for graphene growth on Cu can result in high purity, high quality films, these methods are generally incompatible with equipment used to perform fundamental studies in this field. In particular, the high partial and total pressures required for the sample growth are generally not feasible in ultra-high vacuum systems that are commonly utilized with such techniques. For example, x-ray standing wave measurements of graphene on Ru,<sup>10</sup> Ir,<sup>11</sup> and SiC<sup>12</sup> are all published in the literature, yet for the far more industrially important graphene on copper, no such experiments have been reported.

To enable *in situ* UHV growth of graphene on copper, we propose a shift away from the frequently used small precursor molecules toward larger polycyclic aromatic hydrocarbons (PAHs)<sup>13</sup> with the aim of increasing the level of control and cleanliness that can be exerted over the growth process.

With our approach, we try to fill a gap between the traditional small-molecule CVD methods, as mentioned above, and the “on-surface synthesis” methods using large, functionalized aromatic molecules as precursors. On-surface synthesis, employing scanning probe microscopy techniques to provide molecular-level spatial characterization, has recently provided an alternative route to the growth of low-dimensional carbon-based nanostructures.<sup>14</sup> Such work is often performed under ultra-high vacuum conditions and has mainly been focused on the synthesis of 1D graphene nanoribbons<sup>15</sup> (as opposed to 2D graphene). These studies often utilize molecular precursors functionalized with specific chemical leaving groups (e.g., halides for Ullman coupling<sup>16</sup>), which aid reactivity. One example from the literature shows the low temperature synthesis of graphene using hexabromobenzene as a precursor.<sup>17</sup> While the authors of this study managed to remove the bromine atoms by annealing to higher temperatures, reactive leaving groups like bromine can still contaminate the resulting films and generally require more precise synthesis conditions.<sup>18</sup> Therefore, a cleaner synthetic route using PAH precursors only containing carbon and hydrogen is desirable. Following previous approaches using PAHs like coronene or pentacene to synthesize graphene in the literature,<sup>13,19</sup> we showcase that the growth of graphene on Cu(111) solely based on dehydrogenative C-C coupling is also possible under ultra-high vacuum (UHV) conditions, while using large aromatic molecules.

As precursors, we chose the isomers pyrene and azulopyrene, both polycyclic aromatic molecules with the chemical formula C<sub>16</sub>H<sub>10</sub> [see Figs. 1(a) and 1(b)]. The molecules only differ in their aromatic topology: pyrene possesses an alternant topology<sup>20</sup> consisting of four 6-membered rings, while azulopyrene has a nonalternant topology<sup>20</sup> containing two 5-membered and two 7-membered rings. The difference in the molecular topology between the two molecules has been shown to lead to different electronic properties<sup>21</sup> as well as a different surface chemistry on Cu(111) with azulopyrene forming a significantly stronger bond at the metal–organic interface when compared to pyrene.<sup>22</sup> In this work, however, we observed that at temperatures required for graphene growth, the difference in topology plays no obvious role, and both molecules can be used to obtain the hexagonal graphene lattice with few defects.

Monolayer graphene was prepared by depositing either pyrene or azulopyrene onto a Cu(111) surface held at 1000 K under ultra-high

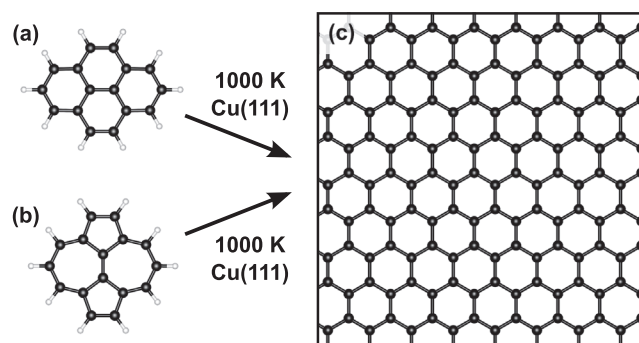


**FIG. 1.** Both pyrene (a) and azulopyrene (b) react to form graphene (c) when deposited onto a Cu(111) surface held at 1000 K. Note that pyrene has an alternant topology with four 6-membered rings, while azulopyrene possesses a non-alternant topology and consists of two 5-membered and two 7-membered rings.

vacuum conditions. Both molecules were deposited onto the substrate using a home-built line-of-sight capillary doser (see Fig. S1 of the [supplementary material](#)). As an advantage of this line-of-sight deposition technique, the pressure in the UHV chamber during deposition could sustainably be kept in the  $10^{-10}$  mbar range. Depending on the precursor and the preparation chamber properties such as the distance between the doser and substrate, deposition between 45 and 60 min resulted in a complete coverage of the Cu(111) surface with graphene (defined here as 1 ML, see Fig. S2 of the [supplementary material](#)). The coverage of the samples was determined using scanning tunneling microscopy (STM) and x-ray photoelectron spectroscopy (XPS), before further characterization. Further experimental details regarding sample preparation and experimental setup can be found in the [supplementary material](#).

Room temperature STM images of graphene films on Cu(111) grown using azulopyrene [Figs. 2(a) and 2(b)] and pyrene [Fig. 3(a)] show island sizes between 75 and 100 nm, where moiré patterns are clearly visible, consistent with observations for graphene on Cu(111) reported in the literature.<sup>23</sup> Over several graphene islands and samples, we observed various moiré patterns with a periodicity between 2.6 and 7.1 nm (see Fig. S3 of the [supplementary material](#)). The larger moiré periodicities likely arise from a structure where the graphene and Cu(111) lattices are rotated with respect to each other by less than  $\sim 2.5^\circ$  in combination with an expansion of the graphene lattice constant of 1%–10%; the smaller moiré periodicities are consistent with a larger angle between the two lattices of about  $\sim 5^\circ$ .<sup>24</sup> Atomically resolved images obtained by low temperature STM (LT-STM,  $T_{\text{sample}} = \sim 79$  K) of a sample grown with azulopyrene as a precursor clearly show the hexagonal honeycomb network of the graphene lattice [Fig. 2(c)].

C 1s high-resolution photoelectron spectra (photon energy 430 eV, taken at the I09 beamline,<sup>25</sup> Diamond Light Source) show a single, narrow peak in the C 1s region, both for samples grown using azulopyrene [Fig. 2(d)] and using pyrene [Fig. 3(c)]. This peak is almost exclusively of Lorentzian shape with a binding energy of 284.6 eV and a full width at half maximum (FWHM) of 0.43 and 0.44 eV for azulopyrene and pyrene grown samples, respectively. The C 1s binding energy agrees well with the previously reported value (284.5 eV) for graphene on Cu(111).<sup>26</sup>

The low-energy electron diffraction (LEED) pattern of the grown networks [azulopyrene: Fig. 2(e), pyrene: Fig. 3(b)] shows a ring

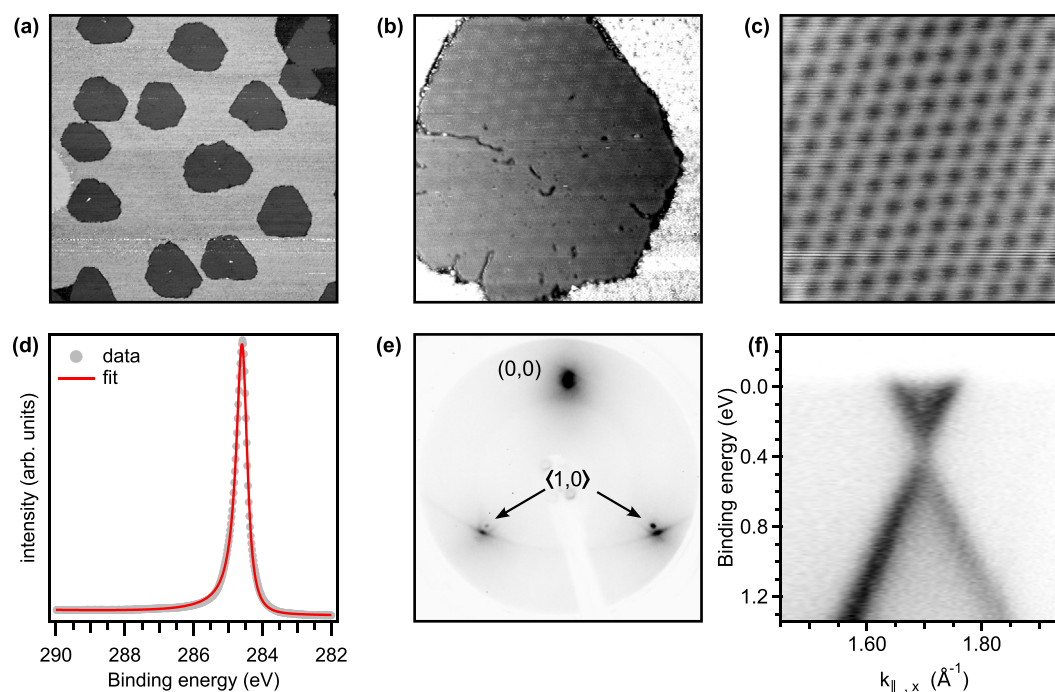


**FIG. 2.** Graphene grown by depositing the azupyrene precursor onto a Cu(111) substrate at 1000 K. (a) Room temperature STM image showing multiple  $\sim 100$  nm graphene islands on a Cu(111) terrace and (b) upon close inspection of an island, a clear moiré pattern is visible. (c) Low temperature STM image showing atomic resolution of the graphene lattice. (d) C 1s XP spectra (photon energy 430 eV) and (e) LEED pattern (63 eV, with indexed substrate reflections) showing a diffuse spot from the graphene flakes near the  $(1,0)$  and  $(0,1)$  spots of Cu(111) as well as a ring stemming from graphene islands in minority orientations. (f) ARPES data (photon energy 21.2 eV) around the K point in reciprocal space show a sharp Dirac cone at 0.35 eV below the Fermi energy. The size of the STM images is  $500 \times 500$  nm<sup>2</sup> for (a),  $90 \times 90$  nm<sup>2</sup> for (b), and  $2.5 \times 2.5$  nm<sup>2</sup> for (c), while the tunneling parameters are  $-1.5$  V, 800 pA for (a) and (b) and  $-1.7$  V, 100 pA for (c).

structure at slightly greater  $|k|$  than the Cu  $\langle 1,0 \rangle$  reflections with a distinct, but diffuse, spot near the Cu reflections, indicating that the majority of the graphene islands are roughly orientated with the Cu substrate (in line with the analysis of the moiré periodicity observed in STM, see the above paragraph), but that overall a continuum of orientations is present. The observed LEED patterns are also consistent with previously reported data for graphene on Cu(111).<sup>5,27</sup>

Angle-resolved photoemission spectroscopy (ARPES) data (photon energy 21.2 eV) clearly show a sharp Dirac cone at the K point in the Brillouin zone of the Cu(111) substrate for samples grown using azupyrene [Fig. 2(f)] and pyrene [Fig. 3(d)]. For the azupyrene sample, the Dirac point is 0.36 eV below the Fermi energy, while it is at 0.38 eV for the pyrene sample. This level of n-doping of graphene on Cu(111) agrees excellently with results previously published in the literature.<sup>28</sup>

*Ex situ* Raman measurements of the azupyrene grown graphene (Fig. 4, excitation wavelength 532 nm) show the presence of the characteristic D, G, D', and 2D bands attributed to graphene.<sup>29,30</sup> The transition causing the intense D-band is only allowed in the presence of defects.<sup>30</sup> In our Raman measurements, the presence of the D-band can be explained by the presence of island boundaries, as the measured sample had a graphene coverage of about 0.7 ML. Furthermore, the Raman measurements were performed in air; therefore, oxidation of the graphene layer, which would also increase the intensity of the D-band, after exposure to air cannot be excluded.<sup>31</sup>

All the above measurements conclusively prove the formation of monolayer graphene by depositing azupyrene or pyrene on Cu(111) at a temperature of 1000 K. As most strikingly visible in our atomically resolved STM measurements [Fig. 2(c)], this finding also clearly demonstrates the presence of the hexagonal graphene lattice [Fig. 1(c)], rather than the irregular pentagonal/heptagonal lattice, which might naively be expected from coupling azupyrene molecules by pure C–H bond scission and C–C bond formation. Therefore, during the formation of the carbon network, the molecular backbone of the azupyrene molecule must undergo some form of C–C rearrangement to transition from the 5–7 topology to the pure hexagonal topology of ideal graphene, which is thermodynamically more stable. This C–C rearrangement has been previously observed as so-called Stone–Wales rearrangement,<sup>32</sup> converting azupyrene to pyrene, with a 40% transformation yield at  $\sim 775$  K (in  $10^{-4}$  Torr of N<sub>2</sub>).<sup>33</sup> Therefore, it is not unreasonable to assume that the Stone–Wales rearrangement would also occur when supported on the catalytically active Cu(111) surface. Rearrangements involving a change in the aromatic topology have also been observed in various other molecules, e.g., the rearrangement of azulene into naphthalene,<sup>34</sup> or involving nanographenes on Au(111)<sup>35</sup> or in a solution.<sup>36</sup>

In conclusion, we have demonstrated the UHV synthesis of high-coverage, low-defect graphene on Cu(111) from polycyclic aromatic hydrocarbons as molecular precursors with the substrate held at lower temperatures than more traditional routes leading to graphene formation on Cu surfaces. The growth is achieved by depositing the

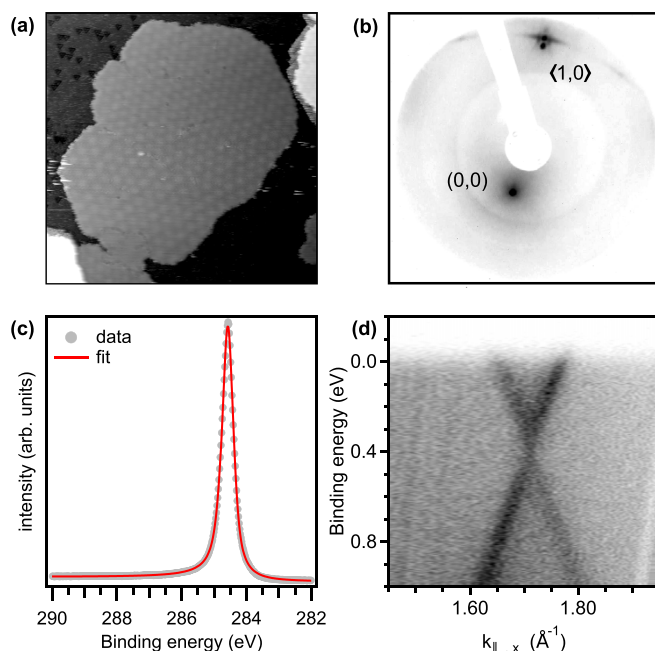


**FIG. 3.** Graphene grown by depositing the pyrene precursor onto a Cu(111) substrate at 1000 K. (a) Room temperature STM image showing a 45 nm graphene island with a clearly visible moiré pattern ( $50 \times 50 \text{ nm}^2$ ,  $-1.5 \text{ V}$ ,  $300 \text{ pA}$ ). (b) LEED pattern ( $70 \text{ eV}$ , with indexed substrate reflections) showing a diffuse spot from the graphene flakes near the (1,0) reflex of Cu(111) as well as a ring stemming from graphene islands in minority orientations. (c) C 1s XP spectra (photon energy  $430 \text{ eV}$ ) with a binding energy of  $284.6 \text{ eV}$  and a FWHM of  $0.44 \text{ eV}$  and (d) ARPES data (photon energy  $21.2 \text{ eV}$ ) around the K point in reciprocal space show a sharp Dirac cone at  $0.35 \text{ eV}$  below the Fermi energy.

PAHs azupyrene or pyrene via a line-of-sight doser onto the Cu(111) substrate held at a temperature of  $1000 \text{ K}$ . The presented method allows the synthesis to take place under highly controlled conditions, enabling stringent fundamental studies into the growth mechanism of graphene on copper. This study serves as a proof of principle that

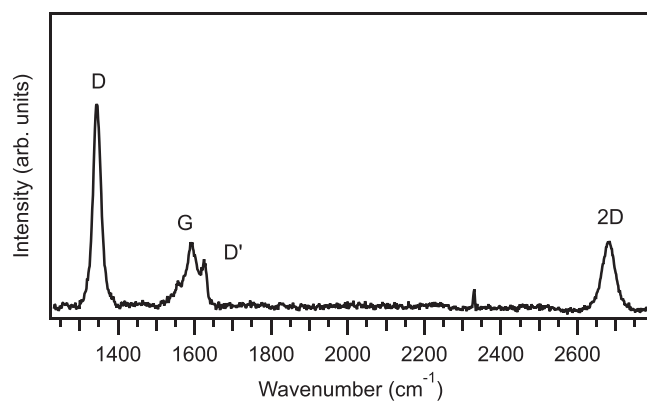


**FIG. 4.** Background subtracted Raman spectrum (photon wavelength  $532 \text{ nm}$ ) of graphene grown from an azupyrene precursor on a Cu(111) substrate. D, G, D', and 2D mark the bands according to nomenclature common in the literature. The sharp signal at  $2330 \text{ cm}^{-1}$  is an instrumental artifact of the detector (a so-called "hot pixel").

growth with PAH precursors could be a viable method for clean production of graphene on copper substrates. There is no obvious reason why this approach should not work on polycrystalline copper foils. On such foils, it seems reasonable for the reaction temperature to be even lower due to the presence of the more reactive (110) and (001) surface facets. Further refinement of our approach could result in a methodology to produce graphene more effectively and more reliably for industrial applications.

See the [supplementary material](#) for additional details on sample preparations and experimental techniques as well as additional STM data.

The authors thank the Diamond Light Source for access to beamline I09 (Nos. SI25379-4 and SI25379-5). B.P.K. acknowledges support from the DFG under the Walter Benjamin Fellowship Programme (No. KL 3430/1-1). M.A.S. acknowledges support from the Analytical Science CDT at the University of Warwick. R.J.M. acknowledges financial support via a UKRI Future Leaders Fellowship (No. MR/S016023/1). A.S. acknowledges support via a Royal Society University Research Fellowship. The authors acknowledge use of the Raman spectrometer as well as the support by Ben Breeze of the Spectroscopy Research Technology Platform, University of Warwick. M.W. acknowledges financial support from the EPSRC-funded Warwick Analytical Science Centre (EP/V007688/1).

## AUTHOR DECLARATIONS

### Conflict of Interest

The authors have no conflicts to disclose.

### Author Contributions

**Benedikt P Klein:** Conceptualization (equal); Formal analysis (lead); Funding acquisition (equal); Investigation (equal); Methodology (equal); Supervision (supporting); Visualization (lead); Writing – original draft (lead); Writing – review & editing (lead). **Tien-Lin Lee:** Formal analysis (equal); Investigation (supporting); Supervision (equal); Visualization (supporting); Writing – review & editing (equal). **Alex Saywell:** Investigation (supporting); Supervision (equal); Writing – review & editing (equal). **Reinhard J Maurer:** Conceptualization (equal); Funding acquisition (equal); Investigation (equal); Project administration (equal); Supervision (equal); Writing – review & editing (equal). **David A Duncan:** Conceptualization (equal); Funding acquisition (equal); Methodology (equal); Project administration (equal); Supervision (equal); Visualization (supporting); Writing – original draft (equal); Writing – review & editing (equal). **Matthew A Stoodley:** Investigation (equal); Writing – review & editing (supporting). **Matthew Edmondson:** Formal analysis (supporting); Investigation (equal). **Luke A Rochford:** Investigation (equal); Methodology (supporting); Supervision (supporting); Writing – review & editing (supporting). **M. Walker:** Investigation (supporting); Writing – review & editing (supporting). **Lars Sattler:** Investigation (supporting); Resources (supporting). **Sebastian M Weber:** Investigation (supporting); Resources (supporting). **Gerhard Hilt:** Investigation (supporting); Resources (supporting); Supervision (equal). **Leon B. S. Williams:** Formal analysis (supporting); Investigation (equal).

## DATA AVAILABILITY

The data that support the findings of this study are available from the corresponding authors upon reasonable request.

## REFERENCES

- <sup>1</sup>L. Lin, H. Peng, and Z. Liu, *Nat. Mater.* **18**(6), 520 (2019).
- <sup>2</sup>Y. Zhu, H. Ji, H.-M. Cheng, and R. S. Ruoff, *Natl. Sci. Rev.* **5**(1), 90 (2018).
- <sup>3</sup>A. Reina, X. Jia, J. Ho, D. Nezich, H. Son, V. Bulovic, M. S. Dresselhaus, and J. Kong, *Nano Lett.* **9**(8), 3087 (2009); K. S. Kim, Y. Zhao, H. Jang, S. Y. Lee, J. M. Kim, K. S. Kim, J.-H. Ahn, P. Kim, J.-Y. Choi, and B. H. Hong, *Nature* **457**(7230), 706 (2009).
- <sup>4</sup>L. Gao, W. Ren, J. Zhao, L.-P. Ma, Z. Chen, and H.-M. Cheng, *Appl. Phys. Lett.* **97**(18), 183109 (2010).
- <sup>5</sup>Z. R. Robinson, P. Tyagi, T. R. Mowll, C. A. Ventrone, and J. B. Hannon, *Phys. Rev. B* **86**(23), 235413 (2012).
- <sup>6</sup>B. Wu, D. Geng, Y. Guo, L. Huang, Y. Xue, J. Zheng, J. Chen, G. Yu, Y. Liu, L. Jiang, and W. Hu, *Adv. Mater.* **23**(31), 3522 (2011).
- <sup>7</sup>L. Zhao, K. T. Rim, H. Zhou, R. He, T. F. Heinz, A. Pinczuk, G. W. Flynn, and A. N. Pasupathy, *Solid State Commun.* **151**(7), 509 (2011).
- <sup>8</sup>W. M. Haynes, *CRC Handbook of Chemistry and Physics* (CRC Press, Boca Raton, 2017), p. 4.
- <sup>9</sup>K. Celebi, M. T. Cole, J. W. Choi, F. Wycizisk, P. Legagneux, N. Rupasinghe, J. Robertson, K. B. K. Teo, and H. G. Park, *Nano Lett.* **13**(3), 967 (2013).
- <sup>10</sup>C. C. Silva, M. Iannuzzi, D. A. Duncan, P. T. P. Ryan, K. T. Clarke, J. T. Küchle, J. Cai, W. Jolie, C. Schlueter, T.-L. Lee, and C. Busse, *J. Phys. Chem. C* **122**(32), 18554 (2018).
- <sup>11</sup>A. T. N'Diaye, J. Coraux, T. N. Plasa, C. Busse, and T. Michely, *New J. Phys.* **10**(4), 043033 (2008).
- <sup>12</sup>J. Sforzini, L. Nemeč, T. Denig, B. Stadtmüller, T. L. Lee, C. Kumpf, S. Soubatch, U. Starke, P. Rinke, V. Blum, F. C. Bocquet, and F. S. Tautz, *Phys. Rev. Lett.* **114**(10), 106804 (2015).
- <sup>13</sup>X.-Y. Wang, X. Yao, and K. Müllen, *Sci. China Chem.* **62**(9), 1099 (2019).
- <sup>14</sup>D. Han and J. Zhu, *J. Phys.: Condens. Matter* **33**(34), 343001 (2021).
- <sup>15</sup>L. Talirz, P. Ruffieux, and R. Fasel, *Adv. Mater.* **28**(29), 6222 (2016).
- <sup>16</sup>M. Lackinger, *Chem. Commun.* **53**(56), 7872 (2017).
- <sup>17</sup>L. Jiang, T. Niu, X. Lu, H. Dong, W. Chen, Y. Liu, W. Hu, and D. Zhu, *J. Am. Chem. Soc.* **135**(24), 9050 (2013).
- <sup>18</sup>C. Moreno, M. Vilas-Varela, B. Kretz, A. Garcia-Lekue, V. Costache, M. M. Paradinas, M. Panighel, G. Ceballos, O. Valenzuela Sergio, D. Peña, and A. Mugarza, *Science* **360**(6385), 199 (2018).
- <sup>19</sup>X. Wan, K. Chen, D. Liu, J. Chen, Q. Miao, and J. Xu, *Chem. Mater.* **24**(20), 3906 (2012); J. Li, S. Lampart, J. S. Siegel, K.-H. Ernst, and C. Wäckerlin, *ChemPhysChem* **20**(18), 2354 (2019).
- <sup>20</sup>R. B. Mallion and D. H. Rouvray, *J. Math. Chem.* **5**(1), 1–21 (1990).
- <sup>21</sup>B. P. Klein, L. Ruppenthal, S. J. Hall, L. E. Sattler, S. M. Weber, J. Herritsch, A. Jaegermann, R. J. Maurer, G. Hilt, and M. Gottfried, *ChemPhysChem* **22**, 1065 (2021).
- <sup>22</sup>B. P. Klein, A. Ihle, S. R. Kachel, L. Ruppenthal, S. J. Hall, L. E. Sattler, S. M. Weber, J. Herritsch, A. Jaegermann, D. Ebeling, R. J. Maurer, G. Hilt, R. Tonner-Zeuch, A. Schirmeisen, and J. M. Gottfried, *ACS Nano* **16**, 11979 (2022).
- <sup>23</sup>L. Gao, J. R. Guest, and N. P. Guisinger, *Nano Lett.* **10**(9), 3512 (2010); E. Soy, Z. Liang, and M. Trenary, *J. Phys. Chem. C* **119**(44), 24796 (2015).
- <sup>24</sup>K. Hermann, *J. Phys.: Condens. Matter* **24**(31), 314210 (2012).
- <sup>25</sup>T.-L. Lee and D. A. Duncan, *Synchrotron Rad. News* **31**(4), 16 (2018).
- <sup>26</sup>D. Choudhury, B. Das, D. D. Sarma, and C. N. R. Rao, *Chem. Phys. Lett.* **497**(1), 66 (2010).
- <sup>27</sup>K. Takeuchi, S. Yamamoto, Y. Hamamoto, Y. Shiozawa, K. Tashima, H. Fukidome, T. Koitaya, K. Mukai, S. Yoshimoto, M. Suemitsu, Y. Morikawa, J. Yoshinobu, and I. Matsuda, *J. Phys. Chem. C* **121**(5), 2807 (2017).
- <sup>28</sup>S. Gottardi, K. Müller, L. Bignardi, J. C. Moreno-Lopez, T. A. Pham, O. Ivashenko, M. Yablonskikh, A. Barinov, J. Björk, P. Rudolf, and M. Stöhr, *Nano Lett.* **15**, 917 (2015).
- <sup>29</sup>L. M. Malard, M. A. Pimenta, G. Dresselhaus, and M. S. Dresselhaus, *Phys. Rep.* **473**(5), 51 (2009).
- <sup>30</sup>A. C. Ferrari and D. M. Basko, *Nat. Nanotechnol.* **8**(4), 235 (2013).
- <sup>31</sup>E. Yazici, S. Yanik, and M. B. Yilmaz, *Carbon* **111**, 822 (2017).
- <sup>32</sup>R. W. Alder and J. N. Harvey, *J. Am. Chem. Soc.* **126**(8), 2490 (2004).
- <sup>33</sup>A. G. Anderson and L. G. Kao, *J. Org. Chem.* **47**, 3589 (1982).
- <sup>34</sup>M. J. S. Dewar and K. M. J. Merz, *J. Am. Chem. Soc.* **108**, 5142 (1986).
- <sup>35</sup>T. G. Lohr, J. I. Urgel, K. Eimre, J. Liu, M. D. Giovannantonio, S. Mishra, R. Berger, P. Ruffieux, C. A. Pignedoli, R. Fasel, and X. Feng, *J. Am. Chem. Soc.* **142**(31), 13565 (2020).
- <sup>36</sup>Y. Han, Z. Xue, G. Li, Y. Gu, Y. Ni, S. Dong, and C. Chi, *Angew. Chem., Int. Ed.* **59**(23), 9026 (2020).